Parallel Multi-Physics Coupled Simulation of a Midrex Blast Furnace

Xavier Besseron*
Prasad Adhav*
Bernhard Peters*
xavier.besseron@uni.lu
prasad.adhav@uni.lu
bernhard.peters@uni.lu
University of Luxembourg
Esch-sur-Alzette, Luxembourg

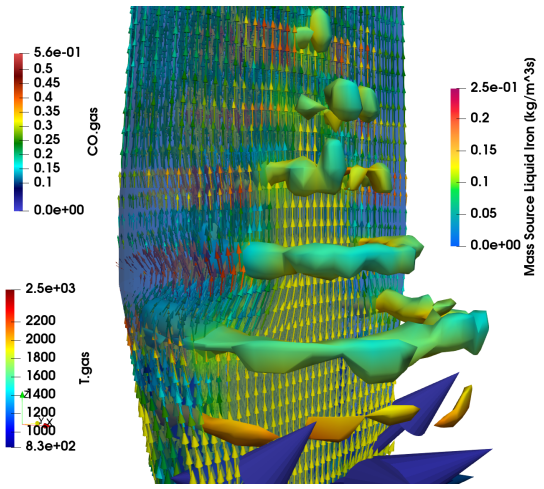

Figure 1: Location of the cohesive zone in a blast furnace simulated by the XDEM simulation platform.

ABSTRACT

Traditional steelmaking is a major source of carbon dioxide emissions, but green steel production offers a sustainable alternative. Green steel is produced using hydrogen as a reducing agent instead of carbon monoxide, which results in only water vapour as a by-product. Midrex is a well-established technology that plays a crucial role in the green steel supply chain by producing direct reduced iron (DRI), a more environmentally friendly alternative to traditional iron production methods.

In this work, we model a Midrex blast furnace and propose a parallel multi-physics simulation tool based on the coupling between Discrete Element Method (DEM) and Computational Fluid Dynamics (CFD). The particulate phase is simulated with XDEM (parallelized with MPI+OpenMP), the fluid phase is solved by OpenFOAM (parallelized with MPI), and the two solvers are coupled together using the preCICE library. We perform a careful performance analysis that focuses first on each solver individually and then on the coupled application. Our results highlight the difficulty of distributing the computing resources appropriately between the solvers in order to achieve the best performance.

Finally, our multi-physics coupled implementation runs in parallel on 1024 cores and can simulate 500 seconds of the Midrex blast furnace in 1 hour and 45 minutes. This work identifies the challenge related to the load balancing of coupled solvers and makes a step forward towards the simulation of a complete 3D blast furnace on High-Performance Computing platforms.

CCS CONCEPTS

• **Applied computing** → **Physical sciences and engineering**; • **Computing methodologies** → **Modeling and simulation**; **Parallel computing methodologies**.

KEYWORDS

extended discrete element method (XDEM), thermal processing, granular material, multi-physics partitioning, multi-physics simulation, CFD-DEM, parallel coupling

*All authors contributed equally to this research.

HPCAsiaWS 2024, January 25–27, 2024, Nagoya, Japan

ACM ISBN 979-8-4007-1652-2/24/01.
https://doi.org/10.1145/3636480.3636484

ACM Reference Format:
Xavier Besseron, Prasad Adhav, and Bernhard Peters. 2024. Parallel Multi-Physics Coupled Simulation of a Midrex Blast Furnace. In *International Conference on High Performance Computing in Asia-Pacific Region Workshops (HPCAsiaWS 2024), January 25–27, 2024, Nagoya, Japan.* ACM, New York, NY, USA, 12 pages. https://doi.org/10.1145/3636480.3636484

1 INTRODUCTION

Traditional steelmaking is the biggest source of carbon dioxide emissions from industry, accounting for 7 % of global CO_2 emissions. Fortunately, there are ways to drastically cut or even eliminate steelmaking emissions and meet the Paris Agreement goals, while also meeting the growing demand for steel.

The transition from traditional steelmaking to green steel represents a revolutionary shift in the metallurgical industry. Standard steel production, largely reliant on carbon-intensive processes like the blast furnace, has long been associated with significant greenhouse gas emissions. In contrast, green steel embodies a sustainable future, emphasizing carbon neutrality and reduced environmental impact. The core of green steel production lies in using hydrogen as a clean reducing agent instead of carbon in traditional coke ovens. This process, known as hydrogen-based direct reduction, emits only water vapour as a by-product. Of course, the green iron produced this way is considered green only if the hydrogen used in the process is itself green.

Midrex is a well-established "green" technology used in the steel industry, specifically in producing direct reduced iron (DRI) or sponge iron. While it may not directly produce green steel, it plays a crucial role in the green steel supply chain by providing a more environmentally friendly alternative to traditional iron production methods.

Midrex technology is known for its:

- Use of Natural Gas: One of the hallmark features of Midrex is its reliance on natural gas as a reducing agent instead of carbon-based materials like coke. This reduces greenhouse gas emissions significantly. The process involves the conversion of iron ore pellets into highly pure and metallic DRI using a combination of natural gas and hydrogen during a transitional period until sufficient hydrogen is available.
- Lower Carbon Footprint: Compared to traditional blast furnace methods, Midrex technology has a substantially lower carbon footprint. By minimizing carbon emissions, it aligns with the goals of green steel production.
- Energy Efficiency: Midrex plants are highly energy-efficient. They can integrate renewable energy sources, such as solar or wind power, into their operations, making them more environmentally sustainable.
- Use of Renewable Hydrogen: In recent years, there has been a growing interest in using renewable hydrogen in the Midrex process. Green hydrogen, produced through electrolysis powered by renewable energy sources, can further reduce the carbon footprint of DRI production.
- Reduced Environmental Impact: The Midrex process emits significantly fewer pollutants, such as sulfur dioxide and nitrogen oxides, compared to traditional steelmaking methods. This contributes to cleaner air quality and reduced environmental harm.
- Flexibility and Modular Design: Midrex plants are known for their flexibility and modular design, which makes them adaptable to various production scales and locations. This adaptability can enable the decentralized production of DRI, reducing the environmental impact associated with transporting raw materials over long distances.

The performance of blast furnaces is evaluated based on their thermal efficiency and harmful emissions, and it is affected by many factors, such as the furnace design and operating conditions. Numerical simulation is a more affordable and time-efficient way to optimize blast furnace operation than expensive experimental methods. For example, as depicted in Figure 1, numerical simulation allows for locating the cohesive zone and thus estimating of the production of liquid iron. However, the Midrex technology in a blast furnace is a complex physical process (involving particle motion and shrinking, heat transfer, reduction, melting and slag formation, etc.) that must be carefully modelled and validated. This high level of complexity means that simulating industrial blast furnaces requires High-Performance Computing (HPC) platforms and expertise to be conducted in a reasonable time.

Our work bridges the gap between chemical engineering and high-performance numerical simulation by providing an advanced high-performance multi-physics simulation of a blast furnace. We present our numerical approach and detail the performance on a High-Performance Computing (HPC) platform. Our contributions, which are novel related to the topic of blast furnace simulations on HPC, are: (1) a parallel multi-physics CFD-DEM coupling application, based on XDEM and OpenFOAM, for the simulation of the Midrex blast furnace; (2) a thorough performance evaluation on an industrial setup, highlighting the challenges related to the load-balancing between coupled solvers.

This paper is organized as follows. First, we present an overview of the state-of-the-art related to the simulations of multi-phase flow phenomena and blast furnaces, and their execution on HPC platforms. Section 3 presents the physical background related to the Midrex process, its validation and parallel implementation with the coupling XDEM–OpenFOAM. A detailed performance evaluation of our solution is carried out in Section 4 and then followed by the Conclusion.

2 RELATED WORKS

Numerical methods for simulating multi-phase flow phenomena involving a solid, like a particulate phase, essentially fall into two categories: The two-fluid model is its most well-known representative, and on a macroscopic level, all phases are treated as a continuum [15]. It is a good fit for process modelling due to its simplicity in computation and effectiveness. The amount of information that can be learned about the material properties, size distribution, or shape of individual particles, however, is significantly diminished by the concept of averaging. To compensate for this loss of information on small scales, additional constitutive or closure relations are needed.

In contrast, the Combined Continuum and Discrete Model (CCDM) treats the flow of liquids or gases as a continuum phase in the interstitial space while treating the solid phase as discrete [20, 61, 71, 72].

Because constitutive relations are excluded from the discrete description of the solid phase, basic ideas are easier to comprehend. This conclusion was reached by Zhu et al. [83] and Zhu et al. [84] while reviewing particulate flows modelled using the CCDM approach. It has undergone significant development over the past decades and treats the other continuous phases while using the Discrete Element Method (DEM) to describe the motion of the solid phase on an individual particle scale. To meet engineering requirements, current models should be expanded to include multi-phase flow behaviour and particle shapes other than spherical geometries, according to Zhu et al. [83] and Zhu et al. [84]. As a result of these efforts, discrete and continuum methods should generally be connected, enabling results to be quantified for process modelling.

At the beginning, only simple flow configurations [20, 61] were handled by the CCDM. However, Chu and Yu [9] demonstrated that the technique could also be used to model complex flow configurations that included a fluidised bed, conveyor belt, and cyclone. Similar to this, Zhou et al. [81] and Chu et al. [8] applied the CCDM approach to the complex geometry of a pulverized coal combustion [81] and Chu et al.[8] modelled the complex of magnetite particles of different sizes in a dense medium cyclone (DMC) including flow of air, water, and coal. In both instances, there was appreciably good agreement between experimental data and predictions. Fluidized beds have also been subject to the CCDM approach, according to reviews by Rowe and Nienow [53] and Feng and Yu [12]. Feng and Yu [12] described the chaotic motion of particles of various sizes in a gas-fluidized bed. See Kafuia et al. [24] for a description of discrete particle-continuum fluid modelling of gas-solid fluidised beds.

The modelling of blast furnaces has also advanced in a similar way. Shibo et al. [26] reviewed recent developments in mathematical modelling related to top charging, shaft processes, raceway, and hearth. Their review indicates that there is still a fragmented approach for isolated regions and physical processes in the blast furnace, such as the studies of combustion in a raceway [16, 50, 59, 65]. Similar to this, Zhou et al. [78] developed numerous computational fluid dynamics (CFD) models for the shaft, raceway, and hearth in order to optimize operating conditions. These shortcomings were partially compensated by a three-dimensional CFD model developed by Lulu et al. [23]. They were successful in achieving a respectable level of agreement between measured and predicted furnace states in both industrial and experimental settings. Dong et al. [14] also employed a CFD model to identify the cohesive zone based on the temperature distribution of the ore. Shen et al. [55] identified key performance indicators like gas utilization and reduction degree using the same CFX-based CFD model. These various models each represent a particular region of a blast furnace, but they largely ignore how those regions interact. However, the current contribution represents an important first step toward a thorough modelling framework that covers the entire blast furnace.

A review by Chattopahyay et al. [5, 6] showed that computational fluid dynamics (CFD) has been employed with great success in many instances as a tool for continuous flow modeling. However, experimental results [17–19, 30–32, 57, 62–64, 67, 74] show that a pure continuous approach to the blast furnace is flawed . For a variety of engineering applications, as discussed by Yu [76], Dong et al. [10] recommend using a discrete approach to model the flow of the solid phase of particles. The CCDM method was used by Simsek et al. [56] to predict grate firing systems, but they only got qualitatively acceptable results, highlighting the need for more research.

Current CCDM approaches should be expanded to a truly multiphase flow behaviour as carried out by [33–35, 39, 48], in contrast to the Volume-of-Fluid method and the multi-phase mixture model. In order to satisfy engineering requirements, it is also necessary to take into account particle shapes other than spherical geometries [36, 40, 68], claim Zhu et al. [83, 84] in their references. Since all derivations have been made for mono-sized particles, as stated by Feng and Yu [11], these efforts should ideally be supplemented by poly-disperse particle systems. For the purposes of process modelling, all of these initiatives should contribute to establishing a general connection between discrete and continuum methodologies.

Even though the CCDM methodology has been in place for more than a decade [61, 71] heat transfer prediction is still in its infancy. The heat transfer for polymerization reactions in gas-fluidised beds was predicted by Kaneko et al. [25] using the Ranz-Marshall correlation [51], but without taking conduction into account. Only in a two-dimensional spouted bed was convective transfer predicted by Swasdisevi et al. [58]. For the transport of gas-solid in horizontal pipes, Li and Mason [27–29] considered conductive heat transfer between particles. Zhou et al. [79, 80] modelled coal combustion in a gas-fluidized bed while taking into account both conductive and convective heat transfer. Although Malone and Xu [38] predicted heat transfer in liquid-fluidized beds by the CCDM method and emphasized the need for further research into heat transfer, Wang et al. [66] predicted the gas-solid flow in a high-density circulating fluidized bed with the two-fluid model. Xiang [69] found during an investigation of air on the packing structure of fine particles that his application lacks computational resources. According to a recent review by Zhou et al. [83] many approaches only take into account flow and ignore heat or mass transfer. Thus, they stated the following recommendations:

- Micro-scale: By developing a more thorough theory and experimental techniques for investigating and calculating the forces that interact with particles and fluids in various environments, we hope to strengthen the groundwork for particle scale simulation [2, 21, 54].
- Macroscale: the development of a general theory that unifies discrete and continuum methods and enables the quantification of particle scale data from DEM or DEM-based simulation in terms of (macroscopic) governing equations [22, 49, 52].
- Application: Transferring the current phenomenon simulation to process simulation is crucial for addressing actual engineering needs. In order to achieve this, it is crucial to create more trustworthy models and efficient computer codes that enable particle scale simulation to be expanded, for example, from a two-phase to a multi-phase and/or from a simple spherical to a complex non-spherical particle system [43–46].

In [77], Zhong et al. highlight that the use of CFD-DEM is not feasible for the simulation of industrial cases because it is too expensive in terms of computation and memory. Indeed, there are no reports of CFD-DEM-based simulation of a complete 3D blast furnace, even in an HPC configuration. The majority of the work used to be based on 2D models [26]. Thanks to the increasing computation power, recent studies propose 3D simulations based on sector model [75] (i.e., one-sixth of a furnace) or sub-part of the system like the raceway [1]. To alleviate the computational needs, scaled methods or coarse-grain approaches have been used for simulation with more than 2 million particles [73]. Unfortunately, authors rarely discuss their implementation, the parallelization or the performance of their simulation prototypes.

More generally, load-balancing has been identified as a critical issue for the performance of multi-physics simulations. In monolithic coupling, solvers are coupled together in a single executable which allows fast in-memory data exchange [47]. This is particularly suitable for volume-coupled problems with the use of a co-located partitioning strategy [47] which assigns the subdomains of the different solvers in the same partition to reduce costly inter-partition inter-physics data exchanges. It has been successfully applied to complex CFD-DEM coupled problems [3, 82]. Alternatively, load-balancing between coupled solvers is achieved by measuring the computational cost of each physics module and then estimating the computation weights [42] to be given to the partitioning algorithm. In partitioned coupling, the configuration is different because each solver can run on a different set of cores. Based on this, [60] builds a performance model of each solver that is used to find the optimal distribution of the computing resources between the solvers.

With the current work, we do not tackle directly load-balacing. Instead, our objective is to study the parallel execution of our Midrex blast furnace implementation and gain insight into its behaviour at large scale. The collected information will serve as a basis for further work related to load balancing.

3 MODELLING AND IMPLEMENTATION OF THE MIDREX BLAST FURNACE

While Midrex technology itself does not directly produce steel products, its role in producing direct reduced iron is a critical step toward green steel production. The DRI produced using Midrex technology can be used as a feedstock in electric arc furnaces (EAFs) or integrated into other steelmaking processes that are more environmentally friendly compared to traditional blast furnaces. As the steel industry continues to transition toward greener and more sustainable practices, technologies like Midrex are expected to play a pivotal role in reducing the industry's carbon emissions and environmental impact, contributing to the development of a more eco-conscious steel sector. Modelling these processes provides insights into heat transfer, fluid dynamics, combustion, and chemical reactions, aiding in furnace design, efficiency enhancement, and emissions reduction. Furnace modelling stands as a dynamic field that intersects engineering, physics, chemistry, and computational science. As industries strive for efficiency, sustainability, and reduced emissions, the role of furnace modelling becomes increasingly pivotal. By addressing challenges and embracing innovative approaches, researchers and industries can collectively drive advancements in this critical realm, shaping the future of iron and steel production. The following Figure 2 depicts a Midrex furnace filled with iron-bearing material.

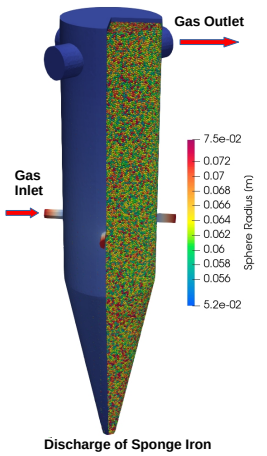

Figure 2: Shape a Midrex furnace filled with iron-bearing particles.

The iron oxides, Magnetite (Fe_3O_4), Hematite (Fe_2O_3), and Wüstite (FeO), undergo reduction with hydrogen and carbon monoxide on the following reaction mechanisms listed in reactions 1 - 6. In particular, reactions 1 - 3 highlight the environmental aspect of the DRI technology avoiding any formation of carbon dioxide and thus, contributing to a significant reduction of the carbon footprint. In the carburizing reaction 7, the iron absorbs methane to produces Cementite (Fe_3C).

Reduction with hydrogen:

$$3Fe_2O_3 + H_2 \leftrightarrow 2Fe_3O_4 + H_2O \quad (1)$$

$$Fe_3O_4 + H_2 \leftrightarrow 3FeO + H_2O \quad (2)$$

$$FeO + H_2 \leftrightarrow Fe + H_2O \quad (3)$$

Reduction with carbon monoxide:

$$3Fe_2O_3 + CO \leftrightarrow 2Fe_3O_4 + CO_2 \quad (4)$$

$$Fe_3O_4 + CO \leftrightarrow 3FeO + CO_2 \quad (5)$$

$$FeO + CO \leftrightarrow Fe + CO_2 \quad (6)$$

Carburizing reaction:

$$3Fe + CH_4 \leftrightarrow Fe_3C + 2H_2 \quad (7)$$

3.1 XDEM and OpenFOAM Coupling

In order to describe the thermal processing of granular material such as iron reduction with the Midrex technology accurately, the particulate phase is represented by discrete entities for which the motion and the thermodynamic state are determined, while the gas phase in the void space between the particles is treated with computational fluid dynamics (CFD) as a continuum approach. Although computationally more expensive than the two-fluid approach or similar approaches solely based on continuum techniques, a coupled Euler-Lagrange coupling is superior due to its accuracy [77]. Therefore, two well-known simulation platforms are chosen for

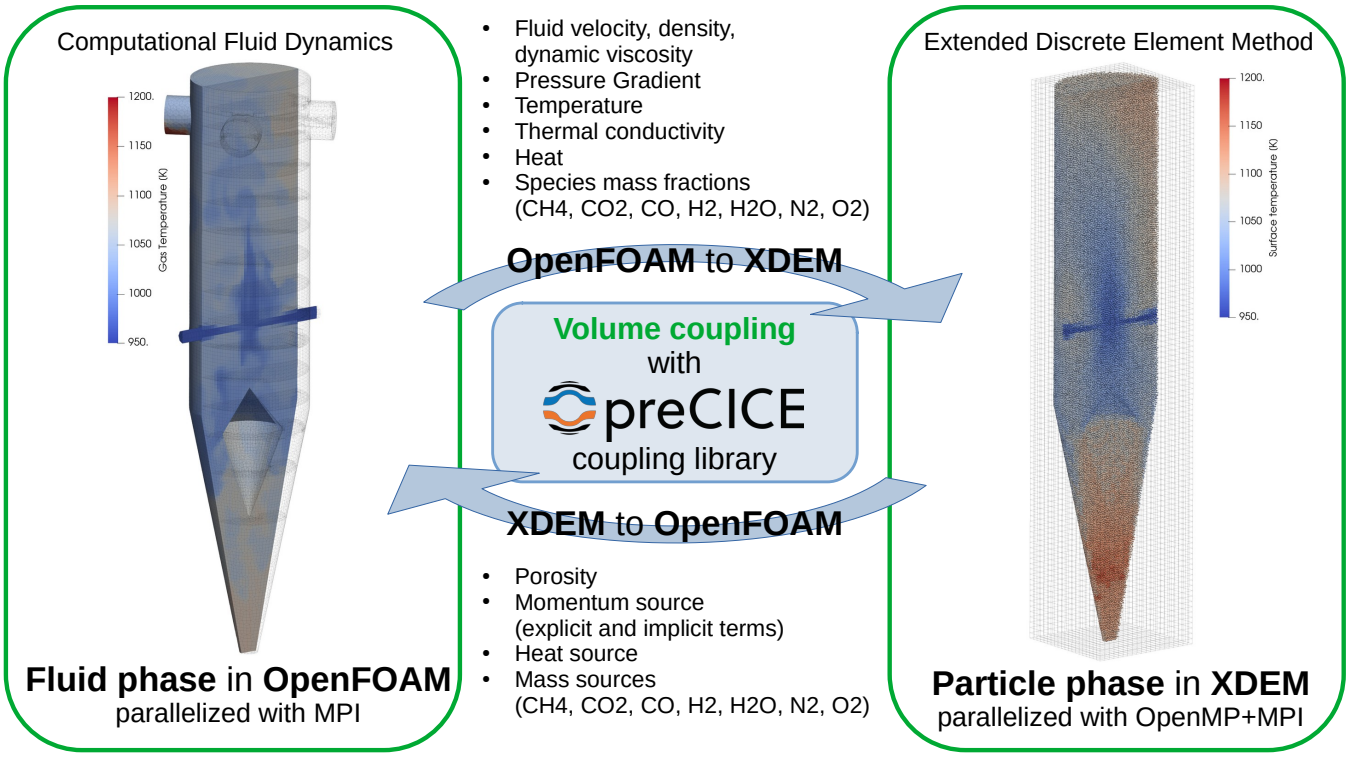

Figure 3: Overview of the Midrex Blast Furnace coupled simulation: The fluid phase is simulated with OpenFOAM (left); the particles are simulated with XDEM (right). The coupling is carried out by the preCICE library (middle) which exchanges the listed physical field values between the two software at every coupling timestep.

coupling, namely the extended discrete element method (XDEM) framework for the discrete phase and OpenFOAM representing CFD. Both modules exchange intensively three quantities: heat, mass and momentum.

- **Heat Exchange**: Particles are heated by the hot incoming gas of approximately 930 °C. Thus, the gas flow transfers heat through a convective transfer to the particles meaning that particles heat up while the gas cools down. These heat quantities are exchanged between the fluid and the particles' surface [4].
- **Mass Exchange**: Particles receive hydrogen and carbon monoxide for reduction from the gas while the gas receives the products vapour and carbon dioxide from the particles. Reducing agents and products are exchanged via particle surfaces through a convective mass transfer [4].
- **Momentum Exchange**: The packed bed and in particular individual particles generate a pressure drop for the flow. Conversely, the gas flow exerts a drag force on particles that is added to other forces, e.g., gravity of the particle. Both transfer directions are accounted for by the momentum transfer [4, 70].

The above-mentioned transfer mechanisms are carried out by the preCICE library [7]. It ensures that individual particles receive the respective fluid quantities according to their position in the CFD simulation domain. Reversely, the fluid has to receive the correct particle properties e.g. surface temperature to account for the above-mentioned quantities transferred. Figure 3 gives an overview of the coupling between XDEM and OpenFOAM. At every coupling timestep, the preCICE coupling library communicates the values of the physical scalar and vector fields between the two solvers. Because the two simulation domains overlap (i.e., the particles are immersed within the fluid and move independently), we have a volume coupling and thus the amount of data to exchange can be quite significant.

3.2 Validation

The implementation of these reactions have been validated over the relevant temperature and composition range as depicted in Figure 4 and 5 using the experimental data collected from [41] and [85]. Most important is that reduction through hydrogen and carbon monoxide as reducing agents is described by two consistent reaction mechanisms with constant kinetic parameters for thermal equilibrium reactions as opposed to fitting each experiment with an individual set of parameters. Predicted reduction degrees agree well with experimental data [41, 85] for all experiments, so these reaction mechanisms are well-suited to be applied to the Midrex furnace.

The following Figures 6 and 7 depict some representative results addressing the temperature and species distribution for the gas phase and particles. The reducing gas is injected through the

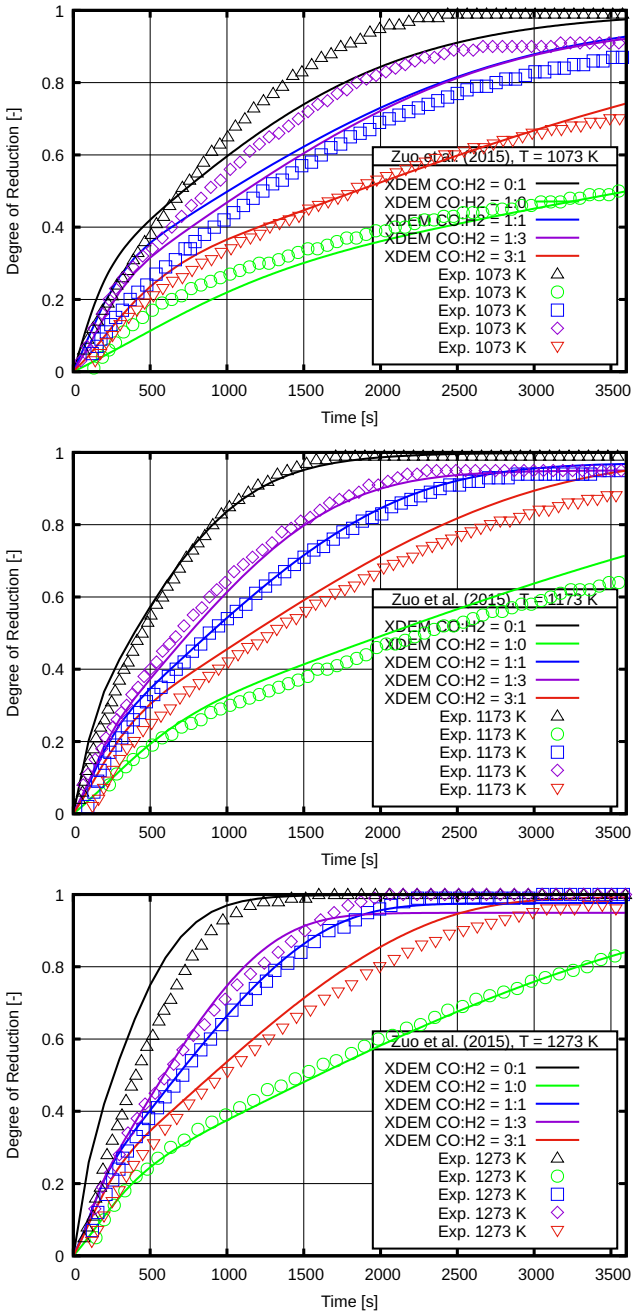

Figure 4: Validation of reducing reactions 1 to 3 for temperatures of 1073 K, 1173 K and 1273 K for different compositions of hydrogen and carbon monoxide in comparison with experimental data from [85].

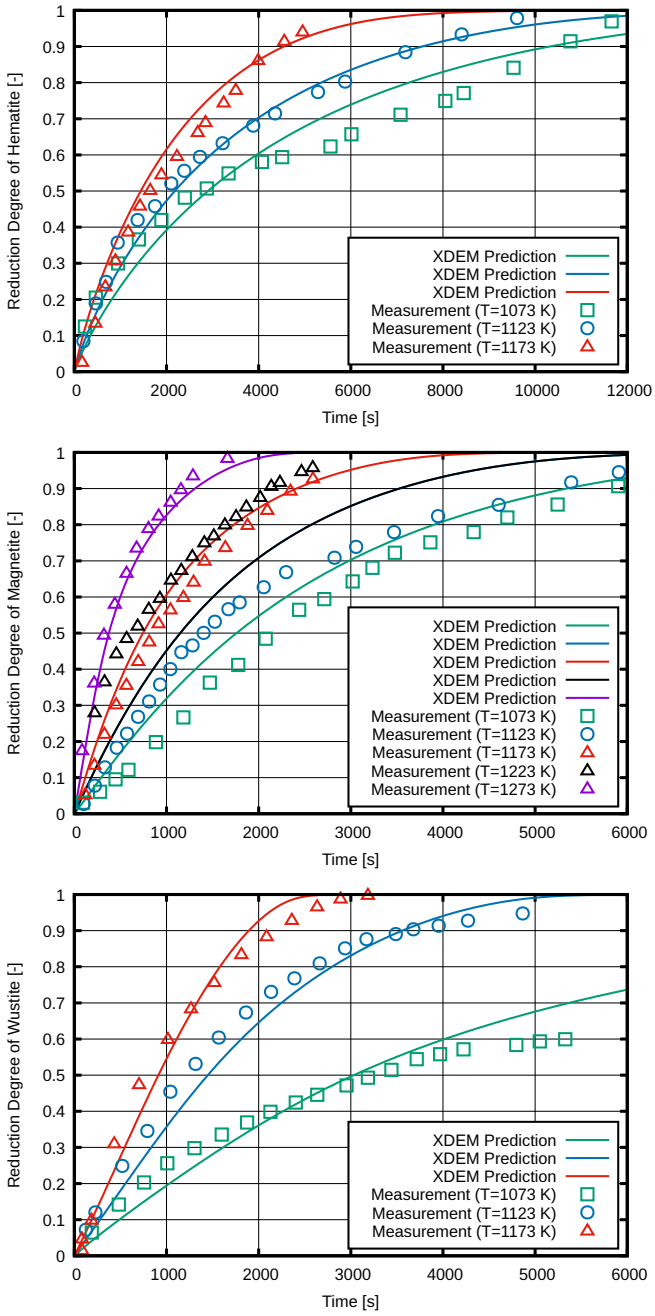

Figure 5: Validation of reducing reactions of Hematite, Magnetite and Wüstite for different temperatures in a pure carbon monoxide atmosphere according to reactions 4 to 6 in comparison with experimental data from [41].

side inlets to stream upward through the packed bed thus, heating the particles and providing the reducing agents meaning that the concentration of hydrogen and carbon monoxide decreases continuously towards the gas outlets. Similarly, the iron oxides of the particles are reduced according to the reactions 1 to 6 so that the particle mass fractions of iron oxide reduce and the mass fraction of iron increases. These detailed results prove the accuracy of the XDEM–CFD coupling and a thorough analysis reveals the underlying physics indispensable for an efficient design and operation.

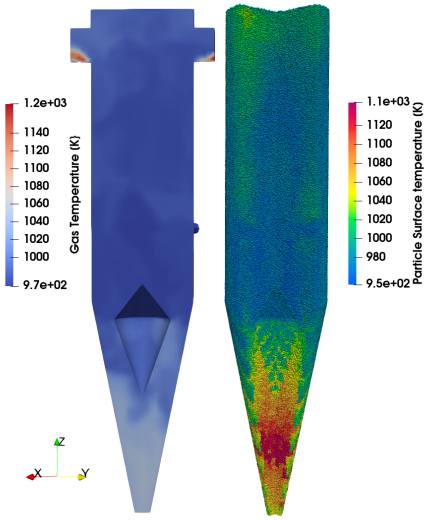

Figure 6: Gas and particle surface temperature distribution in a Midrex furnace.

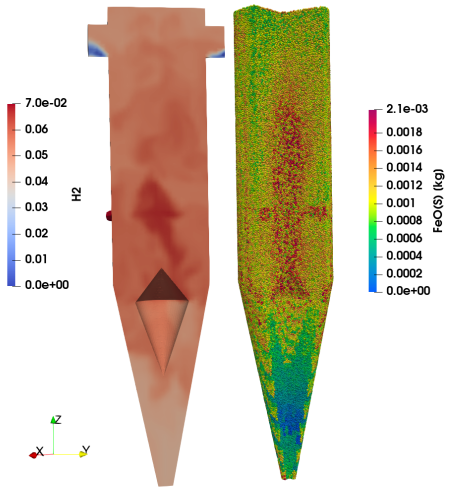

Figure 7: Distribution of hydrogen in the gas phase and progress of reduction represented by the partial mass of iron oxide (FeO) for the particles.

3.3 Parallelisation Approach

The CFD-DEM coupling is a **volume coupling** (as opposed to a surface coupling) because the particles are located and interact with the fluid around them. That means that the amount of data exchanged is proportional to the volume of overlapping domains between CFD and DEM. As discussed in [3, 47], this can have a significant impact on the performance of the execution. Parallelization strategies for single-physics applications such as computational fluid dynamics (CFD), finite element analysis (FEM) or Lattice Boltzmann (LB) are well-developed. However, coupling two or more applications represented by parallelized software modules does not result automatically in a parallelized coupled solver [3].

In our current implementation, we rely on the preCICE coupling library [7] which is designed to support parallel applications based on domain decomposition. With preCICE, each solver is considered a black box. At the initialization, each process of each solver indicates the part of the domain (more precisely, the points of the mesh) that it is responsible for. This has many advantages: First, each solver can run in parallel using its native parallelization scheme (e.g., MPI or OpenMP). Furthermore, the preCICE library takes care of matching the overlapping subdomains between each solver and communicating the data accordingly. Finally, the two solvers can be executed concurrently (*parallel coupling* in the preCICE terminology) and synchronize automatically when data exchange is needed. This approach addresses the main issues highlighted in our previous works [47] and discussed in [3], namely the constraint on the partition alignment and the requirement for inter-partition inter-physics communication.

As a result, we obtain a parallel multi-physics coupled CFD-DEM solver for the Midrex blast furnace that takes advantage of two types of parallelisms [13]: With **functional decomposition**, XDEM and OpenFOAM are executed concurrently, solving respectively the particle phase and the fluid phase. With **domain decomposition**, both XDEM and OpenFOAM are executed in parallel after partitioning their respective domain. In OpenFOAM, the global CFD mesh is decomposed into smaller meshes that are distributed to computing nodes and are solved in parallel using MPI. On its side, XDEM is based on a hybrid OpenMP+MPI approach [37] in which the domain cell grid is decomposed and partitioned into subdomains in order to balance the workload. The subdomains are distributed to the processes and executed in parallel using MPI. Within each process, a fine-grain parallelization takes place at the particle level using OpenMP.

However, in this configuration, each solver runs in parallel and its workload is partitioned using its native implementation. There is no coordination for the partitioning of the two solvers that would account for their relative workload and assign the computing resources proportionally. Because of the synchronization occurring between the solvers at every coupling timestep, the slower solver will slow down the whole simulation. This is the focus of the next section.

4 PERFORMANCE EVALUATION

For the performance evaluation, we consider a Midrex blast furnace as depicted in Figure 2 with a total height of $32m$ and a maximum diameter of $6.5m$. It features 4 gas inlets at the mid-height and 4 gas outlets at the top and the CFD mesh is composed of 133,559 cells. The furnace is filled with 485,336 porous spherical particles with a radius between $4.5cm$ and $7.5cm$ and an internal chemical composition of 12 solid and gaseous species. In order to reduce the computational load, we use a scaling factor of 10 for the particles. This means that each simulated particle represents physical particles 10 times smaller, and the thermodynamic state is solved

accordingly. In addition, for the sake of this study, the particle motion was disabled to avoid changes in the workload distribution over time.

For the software, we used OpenFOAM 7 (Git hash $3bcbaf9$), XDEM (Git hash $d03d01f$), and preCICE 2.5.0. The executions were carried out on the *Aion* cluster of the University of Luxembourg[1] which offers 354 computing nodes, each equipped with 256 GB of memory and two processors AMD Epyc ROME 7H12 2.6 GHz for a total of 128 cores per computing node. Executions were performed with exclusive access to the computing nodes and processes were bound to the computing cores using SLURM.

4.1 Individual Scalability of XDEM and OpenFOAM

We first study the scalability of each solver individually. We consider the coupled simulation of the Midrex blast furnace, but we measure only the time spent in each solver without including the synchronization due to the coupling. For these executions, the processes of XDEM and OpenFOAM are assigned to distinct computing nodes with exclusive access (i.e., only XDEM processes or only OpenFOAM processes on each node). We measure the average time over 500 iterations, and we report the results in Figure 8. With nearly half a million particles and many chemical reactions taking place within the particles, the workload in XDEM is significant. As a result, XDEM displays good scalability with a computing time that continuously decreases up to 512 cores (i.e., four computing nodes). On the other hand, OpenFOAM shows a limited scalability, with a best performance for 16 processes and a computing time that slowly increases beyond that. This is due to the relatively small number of cells in the CFD mesh that limits the workload per process.

For an execution on a single core (not shown in the figure), XDEM requires an average of $41.2s$ per iteration, which is about 42 times more than for OpenFOAM in sequential ($0.98s$). This highlights the significant difference in workload between the two solvers.

4.2 Scalability of coupled XDEM–OpenFOAM

We now focus on the behaviour of the coupled execution, and we measure the coupled iteration time averaged over 500 iterations for XDEM and OpenFOAM running on different set of computing nodes as in the previous study. The coupled iteration time includes the data exchange between the solvers and the synchronization that comes with it. The results are shown in Figure 9. On the left (Figure 9a), the coupled execution time decreases when more computing cores are added to XDEM. This is true until XDEM ceases to be the dominant solver. If OpenFOAM runs on a single core, its iteration time is around $1s$ and there is no benefit in running XDEM on more than 128 cores in this case. On the right, Figure 9b shows the same results from the other perspective, i.e., when increasing the number of cores for OpenFOAM. Assigning more computing resources to OpenFOAM does not reduce the iteration time while the XDEM is the dominant solver. With 128 cores or more assigned to XDEM, there is a benefit in running OpenFOAM in parallel on 2 or 4 cores.

These results show in practice the impact on the performance of the coupling synchronization. The dominant solver is the bottleneck and slows down the execution of the whole simulation. If more computing resources were to be added, they should be assigned to the dominant solver unless it has already reached its performance peak. However, it is important to notice that the dominant solver can change with the newly assigned resources and that this has to be re-evaluated if new cores have to be added again.

[1] https://hpc-docs.uni.lu/systems/aion/

4.3 Complete Simulation of the Midrex Blast Furnace

Finally, we leverage the results of our scalability studies to execute the complete simulation of the Midrex Blast Furnace for 500 seconds. In these executions, the processes of XDEM and OpenFOAM are packed together to fit the defined number of computing nodes, with all the OpenFOAM processes on the same node. In Figure 10, we show the total execution time of the complete simulations at a larger scale. For a given number of cores, we compare side-by-side the time spent in each solver (bright colour) and the time spent in the coupling communication and synchronization (light colour). The different Figures, from left to right (10a, 10b and 10c), show the performance of the coupled execution on 2, 4 and 8 computing nodes respectively.

On the left, Figure 10a shows the results for 2 computing nodes (256 cores) for an increasing number of cores assigned to OpenFOAM (and a slightly decreasing number of cores assigned to XDEM). We can see the switch of the workload between the solvers and how the coupled execution performance is limited by the dominant solver. We observe a similar trend with more computing resources in Figures 10b (512 cores) and Figure 10c (1024 cores), where the execution is dominated either by XDEM or OpenFOAM depending on how many cores they are assigned. The execution time increase of XDEM for the configurations (504+4) and (1016+8) appears to be linked to an unfortunate leap of the load-imbalance in the generated partitions for these specific configurations. This assumption is confirmed by a measured increase of the synchronization time between the XDEM processes at every timesteps.

Regarding the performance of the coupled execution, increasing the number of resources used to solve the problem allows speeding up the simulation if the cores are correctly distributed between the solvers. In the presented results, the best configuration is achieved with 1024 cores (for XDEM running on 1016 cores and OpenFOAM running on 8 cores) and simulates 500 seconds of the Midrex blast furnace in 1 hour and 45 minutes.

Finally, in Figure 10c, running the simulation with 1008 cores for XDEM and 16 cores for OpenFOAM reduces the time spent in each solver individually but it does not reduce the coupled simulation time (in comparison to the 1016+8 configuration). This leads us to believe that, at this scale, the data exchange and the coupling synchronization between the solvers are becoming a bottleneck for the performance of the coupled simulation with about 27% of the total time.

5 CONCLUSION

In this work, we focused on the Midrex blast furnace which has significant advantages in terms of energy efficiency and environmental impact. We presented our modelling and implementation based on XDEM (for the particle phases) and OpenFOAM (for the fluid phase) coupled using the preCICE library. Our implementation

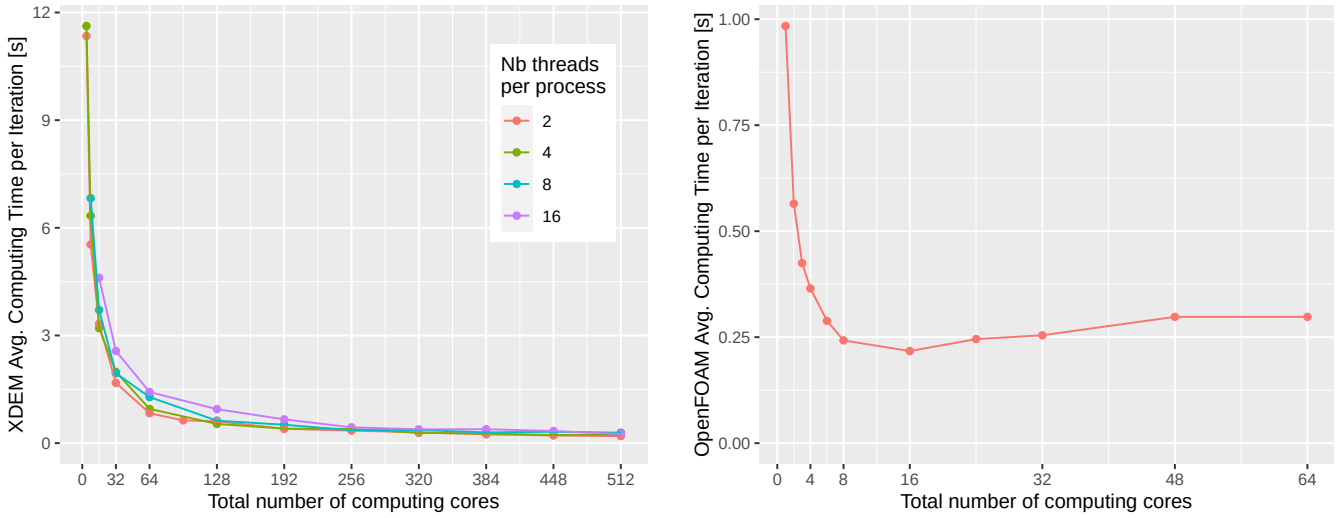

(a) Computing time spent in XDEM

(b) Computing time spent in OpenFOAM

Figure 8: Average iteration time spent purely in XDEM (left) and OpenFOAM (right) in function of the number of cores.

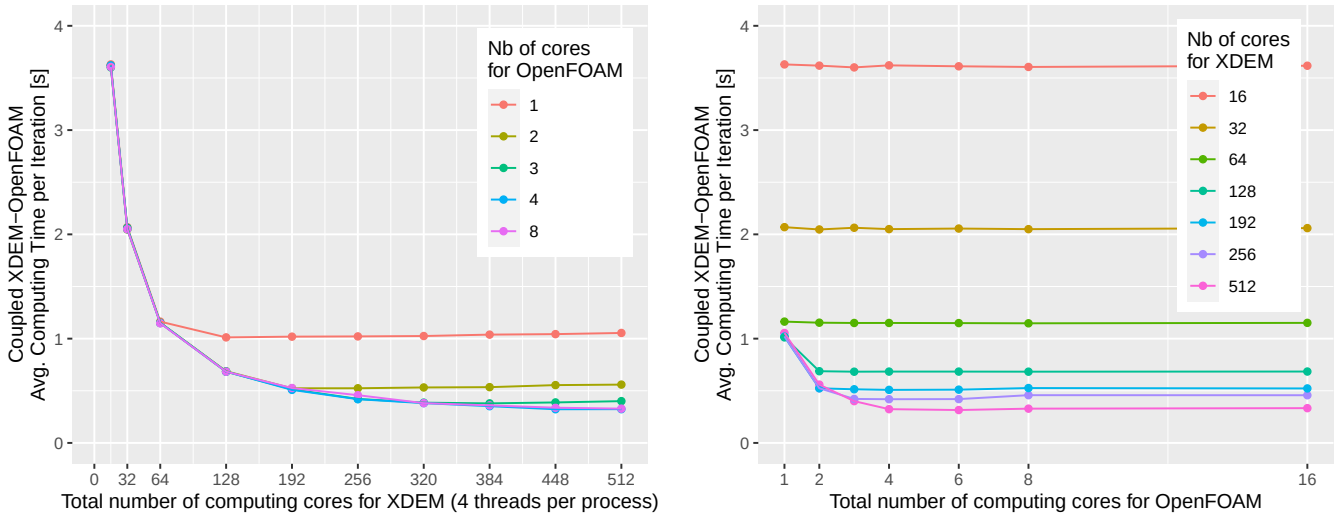

(a) In function of the number of cores assigned to XDEM

(b) In function of the number of cores assigned to OpenFOAM

Figure 9: Average iteration time of the coupled execution XDEM-OpenFOAM.

benefits from functional parallelism (the two solvers run concurrently) and decomposition parallelism (each solver runs in parallel with its native domain decomposition method). More precisely, XDEM relies on hybrid parallelization using MPI+OpenMPI and OpenFOAM is parallelized with MPI.

A thorough performance evaluation has been carried out to study the behaviour of the coupled system under varying numbers of cores. In the best configuration, we achieved a coupled simulation of 500 seconds of our Midrex blast furnace in 1 hour and 45 minutes using 1024 cores.

Our work presents a detailed performance analysis of a complex real-world application employing volume coupling, and provide a concrete report that can guide the design of multi-physics load balancers. Our findings reveal a substantial work imbalance between the CFD and DEM solvers. This underscores the challenges in effectively distributing computing resources among the coupled solvers. Notably, each solver is partitioned independently and balances only the workload of its own physics domain. The load-balancing techniques currently employed fail to account for multi-solver workloads.

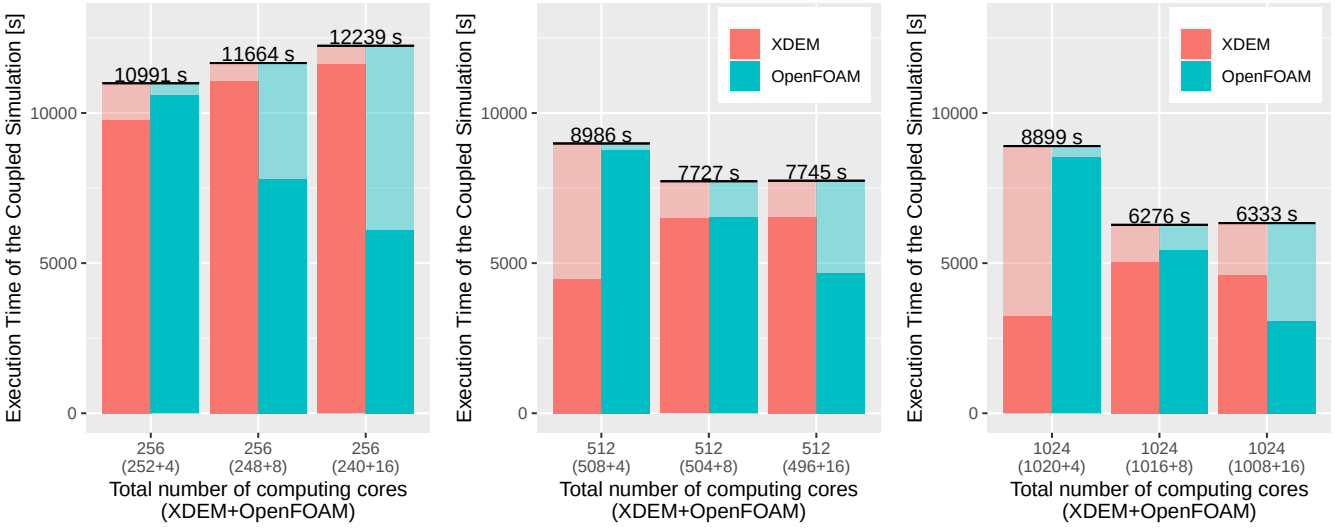

(a) Execution on 2 computing nodes. **(b) Execution on 4 computing nodes.** **(c) Execution on 8 computing nodes.**

Figure 10: Execution time for the simulation of 500s of the Midrex Blast Furnace with coupled XDEM-OpenFOAM. The bright colour represents the time actually spent in the solver and the light colour the time related to coupling communication and synchronization.

We made a step forward for the simulation of complex industrial processes with a multi-physics coupled CFD-DEM approach on HPC platforms. There are many remaining challenges to be addressed for the simulation of a complete 3D blast furnace. Thanks to the available computing resources, we will be able to refine our model, in particular by reducing the scaling factor and enabling the motion of particles. These improvements won't be possible without the development of advanced partitioning and load-balancing techniques for coupled multi-physics problems, which should account for the workload of each physics solver and also their dynamic behaviour.

ACKNOWLEDGMENTS

The authors would like to extend their gratitude to all members, past and current, of the XDEM team who contributed to the Extended Discrete Element Method (XDEM). Furthermore, the Fonds National de la Recherche of Luxembourg are greatly acknowledged for their continuous support. The experiments presented in this paper were carried out using the HPC facilities of the University of Luxembourg – see https://hpc.uni.lu.

REFERENCES

[1] N. Aminnia, P. Adhav, F. Darlik, M. Mashhood, S. Hassanzadeh Saraei, X. Besseron, and B. Peters. 2023. Three-Dimensional CFD-DEM Simulation of Raceway Transport Phenomena in a Blast Furnace. *Fuel* 334 (Feb. 2023), 126574. https://doi.org/10.1016/j.fuel.2022.126574

[2] M. Baniasadi, B. Peters, J.-C. Pierret, B. Vanderheyden, and O. Ansseau. 2018. Experimental and numerical investigation into the softening Behavior of a packed bed of iron ore pellets. *Powder Technology* 339 (2018), 863–871. https://doi.org/10.1016/j.powtec.2018.08.035

[3] X. Besseron, H. Rusche, and B. Peters. 2022. Parallel Multi-Physics Simulation of Biomass Furnace and Cloud-based Workflow for SMEs. In *Practice and Experience in Advanced Research Computing (PEARC)*. https://doi.org/10.1145/3491418.3530294

[4] R. B. Bird, W. E. Stewart, and E. N. Lightfoot. 1960. *Transport Phenomena.* John Wiley & Sons.

[5] K. Chattopadhyay, M. Isac, and R. I. L. Guthrie. 2010. Applications of Computational Fluid Dynamics (CFD) in iron- and steelmaking: Part 1. *Ironmaking and Steelmaking* 37, 8 (2010), 554–561.

[6] K. Chattopadhyay, M. Isac, and R. I. L. Guthrie. 2010. Applications of Computational Fluid Dynamics (CFD) in iron- and steelmaking: Part 2. *Ironmaking and Steelmaking* 37, 8 (2010), 562–569.

[7] G. Chourdakis, K. Davis, B. Rodenberg, M. Schulte, F. Simonis, B. Uekermann, G. Abrams, H. J. Bungartz, L. Cheung Yau, I. Desai, K. Eder, R. Hertrich, F. Lindner, A. Rusch, D. Sashko, D. Schneider, A. Totounferoush, D. Volland, P. Vollmer, and O. Z. Koseomur. 2022. preCICE v2: A sustainable and user-friendly coupling library [version 2; peer review: 2 approved]. *Open Research Europe* 2, 51 (2022). https://doi.org/10.12688/openreseurope.14445.2

[8] K. W. Chu, B. Wang, A. B. Yu, A. Vince, G. D. Barnett, and P. J. Barnett. 2009. CFD-DEM study of the effect of particle density distribution on the multiphase flow and performance of dense medium cyclone. *Minerals Engineering* 22 (2009), 893–909.

[9] K. W. Chu and A. B. Yu. 2008. Numerical simulation of complex particle-fluid flows. *Powder Technology* 179 (2008), 104–114.

[10] Xuefeng Dong, Aibing Yu, Jun ichiro Yagi, and Paul Zulli. 2007. Modelling of Multiphase Flow in a Blast Furnace: Recent Developments and Future Work. *ISIJ International* 47, 11 (2007), 1553–1570. 3.

[11] Y. Q. Feng and A. B. Yu. 2004. Assessment of model formulations in the discrete particle simulation of gas-solid flow. *Industrial & Engineering Chemistry Research* 43 (2004), 8378–8390.

[12] Y. Q. Feng and A. B. Yu. 2008. An analysis of the chaotic motion of particles of different sizes in a gas fluidized bed. *Particuology* 6 (2008), 549–556.

[13] Ian Foster. 1995. *Designing and Building Parallel Programs: Concepts and Tools for Parallel Software Engineering.* USA.

[14] D. Fu, Y. Chen, Y. Zhao, J. D'Alessio, K. J. Ferron, and C. Q. Zhou. 2014. CFD modeling of multiphase reacting flow in blast furnace shaft with layered burden. *Applied thermal engineering* 66, 1-2 (2014), 298–308.

[15] D. Gidaspow. 1994. *Multiphase flow and Fluidisation.* Academic Press.

[16] T. Grejtak, S. Wang, and J. Shao. 2022. Modeling of a Blast Furnace with Both CFD and Thermodynamics Principles. *Applied Mechanics* 3, 3 (2022), 1019–1039.

[17] G. Gupta, J. D. Litster, and V. R. Rudolph. 1996. Model Studies of Liquid Flow in the Blast Furnace Lower Zone. *Journal of Iron And Steel Research, International* 36 (1996), 32–39.

[18] G. Gupta, J. D. Litster, E. T. White, and V. R. Rudolph. 1997. Nonwetting Flow of a Liquid Through a Packed Bed With Gas Cross-Flow. *Metallurgical and Materials Transactions B* 28B (1997), 597–604.

[19] G. S. Gupta, J. D. Litster, V. R. Rudolph, and E. T. White. 1994. A cold model study of liquid flow in the Blast Furnace lower zone. In *6th AusIIM Extractive Metallurgy Conference, Brisbane, 3-6 July 1994.* 295–301.

[20] B. P. B. Hoomans, J. A. M. Kuipers, W. J. Briels, and W. P. M. Van Swaaij. 1996. Discrete Particle Simulation of Bubble and Slug Formation in a Two-dimensional Gas-fluidized Bed: A Hard-Sphere Approach. *Chem. Eng. Sci.* 51 (1996).

[21] C. Introini, D. Baroli, S. Lorenzi, A. Cammi, S. Bordas, and B. Peters. n.d.. A mass conservative Kalman filter algorithm for thermo-computational fluid dynamics. *Materials (ISSN 1996-1944)* (n.d.). http://hdl.handle.net/10993/36124

[22] C. Introini, A. Cammi, S. Lorenzi, D. Baroli, and B. Peters. 2018. Development of a Data-Driven Approach based on Kalman filtering for CFD Reactor Analysis. *PHYSOR 2018* (2018). http://hdl.handle.net/10993/36125

[23] L. Jiao, S. Kuang, A. Yu, Y. Li, X. Mao, and H. Xu. 2020. Three-Dimensional Modeling of an Ironmaking Blast Furnace with a Layered Cohesive Zone. *Metallurgical and materials transactions. B, Process metallurgy and materials processing science* 51, 1 (2020), 258–275.

[24] K. D. Kafuia, C. Thornton, and M. J. Adams. 2002. Discrete particle-continuum fluid modelling of gas-solid fluidised beds. *Chemical Engineering Science* 57 (2002), 2395–2410.

[25] Y. Kaneko, T. Shiojima, and M. Horio. 1999. DEM simulation of fluidized beds for gas-phase olefin polymerization. *Chemical Engineering Science* 54 (1999), 5809.

[26] S. Kuang, Z. Li, and A. Yu. 2018. Review on Modeling and Simulation of Blast Furnace. *Steel research international* 89, 1 (2018), 1700071–n/a.

[27] J. T. Li and D. J. Mason. 2000. A computational investigation of transient heat transfer in pneumatic transport of granular particles. *Powder Technology* 112 (2000), 273.

[28] J. T. Li and D. J. Mason. 2002. Application of the discrete element modelling in air drying of particulate solids. *Drying Technology* 20 (2002), 255.

[29] J. T. Li, D. J. Mason, and A. S. Mujumdar. 2003. A numerical study of heat transfer mechanisms in gas-solids flows through pipes using a coupled CFD and DEM model. *Drying Technology* 21 (2003), 1839.

[30] D. Y. Liu, G. X. Wang, and J. D. Litster. 2002. Unsaturated Liquid Percolation Flow Through Nonwetted Packed Beds. *AIChE Journal* 48 (2002), 953–962.

[31] D. Y. Liu, S. Wijeratne, and J. D. Litster. 1998. *Scand. J. Metall.* 26 (1998), 79.

[32] P.J. Mackey and N.A. Warner. 1973. Studies in the vaporization of mercury in irrigated packed beds. *Chemical Engineering Science* 28 (1973), 2141–2154.

[33] A. H. Mahmoudi, X. Besseron, F. Hoffmann, M. Markovic, and B. Peters. 2016. Modeling of the biomass combustion on a forward acting grate using XDEM. *Chemical Engineering Science* 142 (2016), 32–41. https://doi.org/10.1016/j.ces.2015.11.015

[34] A. H. Mahmoudi, F. Hoffmann, and B. Peters. 2014. Application of XDEM as a novel approach to predict drying of a packed bed. *International Journal of Thermal Sciences* 75 (2014), 65e75. http://hdl.handle.net/10993/6363

[35] A. H. Mahmoudi, F. Hoffmann, and B. Peters. 2014. Detailed numerical modeling of pyrolysis in a heterogeneous packed bed using XDEM. *Journal of Analytical and Applied Pyrolysis* 106 (2014), 9–20. http://hdl.handle.net/10993/15828

[36] A. H. Mahmoudi, F. Hoffmann, B. Peters, and X. Besseron. 2016. Numerical study of the influence of particle size and packing on pyrolysis products using XDEM. *International Communications in Heat & Mass Transfer* 71 (2016), 20–34. https://doi.org/10.1016/j.icheatmasstransfer.2015.12.011

[37] A. W. Mainassara Chekaraou, A. Rousset, X. Besseron, S. Varrette, and B. Peters. 2018. Hybrid MPI+OpenMP Implementation of eXtended Discrete Element Method. In *2018 30th International Symposium on Computer Architecture and High Performance Computing (SBAC-PAD).* 450–457. https://doi.org/10.1109/CAHPC.2018.8645880

[38] K. F. Malone and B. H. Xu. 2008. Particle-scale simulation of heat transfer in liquid-fluidised beds. *Powder Technology* 184 (2008), 189–204.

[39] M. Mohseni, A. Kolomijtschuk, B. Peters, and M. Demoulling. 2019. Biomass drying in a vibrating fluidized bed dryer with a Lagrangian-Eulerian approach. *International Journal of Thermal Sciences* 138 (2019), 219 – 234. https://doi.org/10.1016/j.ijthermalsci.2018.12.038

[40] M. Mohseni, B. Peters, and M. Baniasadi. 2017. Conversion analysis of a cylindrical biomass particle with a DEM-CFD coupling approach. *Case Studies in Thermal Engineering* 10 (2017). http://hdl.handle.net/10993/35941

[41] T. Murayama, Y. Ono, and Y. Kawai. 1978. Step-Wise Reduction of Hematite Pellets with CO-CO_2 Gas Mixtures. *Transactions of the Iron and Steel Institute of Japan* 18, 9 (1978), 579–587. https://doi.org/10.2355/isijinternational1966.18.579

[42] A. Niemöller, M. Schlottke-Lakemper, M. Meinke, and W. Schröder. 2020. Dynamic Load Balancing for Direct-Coupled Multiphysics Simulations. *Computers & Fluids* 199 (March 2020), 104437. https://doi.org/10.1016/j.compfluid.2020.104437

[43] B. Peters. 2003. Characterization of Municipal Solid Waste Combustion in a Grate Furnace. *Waste Management* vol. 23/8 (2003), 689–701. http://hdl.handle.net/10993/6019

[44] B. Peters. 2013. The extended discrete element method (XDEM) for multi-physics applications. *Scholarly Journal of Engineering Research* 2 (2013), 1–20. http://hdl.handle.net/10993/4909

[45] Bernhard Peters, Maryam Baniasadi, Mehdi Baniasadi, Xavier Besseron, Alvaro Estupinan Donoso, Mohammad Mohseni, and Gabriele Pozzetti. 2018. XDEM multi-physics and multi-scale simulation technology: Review of DEM-CFD coupling, methodology and engineering applications. *Particuology* (2018). https://doi.org/10.1016/j.partic.2018.04.005

[46] B. Peters, X. Besseron, A. A. A. Estupinan Donoso, F. Hoffmann, M. Michael, and A. H. Mahmoudi. 2013. Enhanced Thermal Process Engineering by the Extended Discrete Element Method (XDEM). *Universal Journal of Engineering Science* 1 (2013), 139–145. http://hdl.handle.net/10993/11445

[47] G. Pozzetti, X. Besseron, A. Rousset, and B. Peters. 2018. A Co-Located Partitions Strategy for Parallel CFD–DEM Couplings. *Advanced Powder Technology* 29, 12 (Dec. 2018), 3220–3232. https://doi.org/10.1016/j.apt.2018.08.025

[48] G. Pozzetti and B. Peters. 2018. A Multiscale DEM-VOF Method for the simulation of three-phase flows. *International Journal of Multiphase Flow* 99 (2018), 186–204. https://doi.org/10.1016/j.ijmultiphaseflow.2017.10.008

[49] F. Qi, S. Kiesgen de Richter, M. Jenny, and B. Peters. 2020. DEM simulation of dense granular flows in a vane shear cell: Kinematics and rheological laws. *Powder Technology* 366 (2020), 722–735. https://doi.org/10.1016/j.powtec.2020.03.008

[50] A.G. Radjuk, A.E. Titlianov, and M.M. Skripalenko. 2017. Computer simulation of temperature field of blast furnace's air tuyere. *Computer Research and Modeling* 9, 1 (2017), 117–125.

[51] W. E. Ranz and W. R. Marshall. 1952. Evaporation from drops. *Chemical Engineering Progress* 48 (1952), 141.

[52] T. Rosemann, B. Kravets, S.R. Reinecke, H. Kruggel-Emden, M. Wu, and B. Peters. 2019. Comparison of numerical schemes for 3D lattice Boltzmann simulations of moving rigid particles in thermal fluid flows. *Powder Technology* 356 (2019), 528–546. https://doi.org/10.1016/j.powtec.2019.07.054

[53] P. N. Rowe and A. W. Nienow. 1976. Particle mixing and segregation in gas fluidized beds—A review. *Powder Technology* 15 (1976), 141–147.

[54] S. Hassanzadeh Saraei and B. Peters. 2023. Immersed boundary method for considering lubrication effects in the CFD-DEM simulations. *Powder Technology* (2023), 118603. https://doi.org/10.1016/j.powtec.2023.118603

[55] Yansong Shen, Baoyu Guo, Sheng Chew, Peter Austin, and Aibing Yu. 2015. Three-Dimensional Modeling of Flow and Thermochemical Behavior in a Blast Furnace. *Metallurgical and materials transactions. B, Process metallurgy and materials processing science* 46, 1 (2015), 432–448.

[56] E. Simsek, B. Brosch, S. Wirtz, V. Scherer, and F. Krüll. 2009. Numerical simulation of grate firing systems using a coupled CFD/discrete element method (DEM). *Powder Technology* 193 (2009), 266–273.

[57] N. Standish. 1968. Dynamic holdup in liquid metal irrigated packed beds. *Chemical Engineering Science* 23 (1968), 51–56.

[58] T. Swasdisevi, W. Tanthapanichakoon, T. Charinpanitkul, T. Kawaguchi, and T. Tsuji. 2005. Prediction of gas-particle dynamics and heat transfer in a two-dimensional spouted bed. *Advanced Powder Technology* 16 (2005), 275.

[59] H. Tang, F. Meng, Z. Zhao, and L. Zhang. 2015. Modeling Coal/coke Combustion Behavior in Tuyere-raceway-dripping Zone in Blast Furnace. *Procedia Engineering* 102 (2015), 1583–1592.

[60] A. Totounferoush, N. Ebrahimi Pour, J. Schröder, S. Roller, and M. Mehl. 2021. A Data-Based Inter-Code Load Balancing Method for Partitioned Solvers. *Journal of Computational Science* 51 (April 2021), 101329. https://doi.org/10.1016/j.jocs.2021.101329

[61] Y. Tsuji, T. Kawaguchi, and T. Tanaka. 1993. Discrete Particle Simulation of Two-dimensional Fluidized Bed. *Powder Technol.* 77, 79 (1993).

[62] G. X. Wang, S. J. Chew, A. B. Yu, and P. Zulli. 1997. Model study of liquid flow in blast furnace lower zone. *Iron and Steel Institute of Japan (ISIJ-International)* 37 (1997), 573–582.

[63] G. X. Wang, S. J. Chew, A. B. Yu, and P. Zulli. 1997. Modeling the Discontinuous Liquid Flow in a Blast Furnace. *Metallurgical and Materials Transactions B* 28B (1997), 333–342.

[64] G. X. Wang, D. Y. Liu, J. D. Litster, A. B. Yu, S. J. Chew, and P. Zulli. 1997. Experimental and Numerical Simulation of Discrete Liquid Flow in a Packed Bed. *Chemical Engineering Science* 52 (1997), 4013–4019.

[65] S. Wang and Y. Shen. 2021. CFD-DEM modelling of raceway dynamics and coke combustion in an ironmaking blast furnace. *Fuel (Guildford)* 302 (2021), 121167–.

[66] X. Wang, F. Jiang, J. Lei, J. Wang, S. Wang, X. Xu, and Y. Xiao. 2011. A Revised Drag Force Model and the Application for the Gas-Solid Flow in the High-density Circulating Fluidized Bed. *Applied Thermal Engineering* 31, 14-15 (2011), 2254–2261.

[67] N. A. Warner. 1959. Liquid metal irrigation of a packed bed. *Chemical Engineering Science* 11 (1959), 149–160.

[68] M. Wu, B. Peters, T. Rosemann, and H. Kruggel-Emden. 2020. A forcing fictitious domain method to simulate fluid-particle interaction of particles with super-quadric shape. *Powder Technology* 360 (2020), 264–277. https://doi.org/10.1016/j.powtec.2019.09.088

[69] J. Xiang. 2009. The effect of air on the packing structure of fine particles. *Powder Technology* 191 (2009), 280–293.

[70] H. Xiao and J. Sun. 2011. Algorithms in a Robust Hybrid CFD-DEM Solver for Particle-Laden Flows. *Communications in Computational Physics* 9, 2 (Feb. 2011), 297–323. https://doi.org/10.4208/cicp.260509.230210a

[71] B. H. Xu and A. B. Yu. 1997. Numerical simulation of the gas-solid flow in a fluidized bed by combining discrete particle method with Computational Fluidd Dynamics. *Chemical Engineering Science* 52 (1997), 2785.

[72] B. H. Xu and A. B. Yu. 1998. Comments on the paper "Numerical simulation of the gas-solid flow in a fluidized bed by combining discrete particle method with computational fluid dynamics?-Reply. *Chemical Engineering Science* 53 (1998), 2646–2647.

[73] D. Xu, S. Wang, and Y. Shen. 2023. An Improved CFD-DEM Modelling of Raceway Dynamics and Coke Combustion in an Industrial-Scale Blast Furnace. *Chemical Engineering Journal* 455 (Jan. 2023), 140677. https://doi.org/10.1016/j.cej.2022.140677

[74] J. Yagi. 1993. Mathematical Modeling of the Flow of Four Fluids in a Packed Bed. *Journal of Iron And Steel Research, International* 33 (1993), 619–639.

[75] W. J. Yang, Z. Y. Zhou, and A. B. Yu. 2015. Discrete Particle Simulation of Solid Flow in a Three-Dimensional Blast Furnace Sector Model. *Chemical Engineering Journal* 278 (Oct. 2015), 339–352. https://doi.org/10.1016/j.cej.2014.11.144

[76] A. B. Yu. 2005. *Encyclopedea of Condensed Matter Physics.* Elsevier, Chapter Powder Processing: Models and Simulations, 401–414.

[77] W. Zhong, A. Yu, G. Zhou, J. Xie, and H. Zhang. 2016. CFD Simulation of Dense Particulate Reaction System: Approaches, Recent Advances and Applications. *Chemical Engineering Science* 140 (Feb. 2016), 16–43. https://doi.org/10.1016/j.ces.2015.09.035

[78] C. Zhou, G. Tang, J. Wang, D. Fu, T. Okosun, A. Silaen, and B. Wu. 2016. Comprehensive Numerical Modeling of the Blast Furnace Ironmaking Process. *JOM (1989)* 68, 5 (2016), 1353–1362.

[79] H. Zhou, G. Flamant, and D. Gauthier. 2004. DEM-LES of coal combustion in a bubbling fluidized bed. Part I: gas-particle turbulent flow structure. *Chemical Engineering Science* 59 (2004), 4193.

[80] H. Zhou, G. Flamant, and D. Gauthier. 2004. DEM-LES simulation of coal combustion in a bubbling fluidized bed. Part II: coal combustion at the particle level. *Chemical Engineering Science* 59 (2004), 4205.

[81] H. Zhou, G. Mo, J. Zhao, and K. Cen. 2011. DEM-CFD simulation of the particle dispersion in a gas-solid two-phase flow for a fuel-rich/lean burner. *Fuel* 90 (2011), 1584–1590.

[82] A. Zhu, Q. Chang, J. Xu, and W. Ge. 2023. A Dynamic Load Balancing Algorithm for CFD–DEM Simulation with CPU–GPU Heterogeneous Computing. *Powder Technology* 428 (Oct. 2023), 118782. https://doi.org/10.1016/j.powtec.2023.118782

[83] H. P. Zhu, Z. Y. Zhou, R. Y. Yang, and A. B. Yu. 2007. Discrete particle simulation of particulate systems: Theoretical developments. *Chemical Engineering Science* 62 (2007), 3378 – 3396.

[84] H. P. Zhu, Z. Y. Zhou, R. Y. Yang, and A. B. Yu. 2008. Discrete particle simulation of particulate systems: A review of major applications and findings. *Chemical Engineering Science* 63 (2008), 5728–5770.

[85] Hb. Zuo, C. Wang, Jj. Dong, Kx. Jiao, and Rs. Xu. 2015. Reduction Kinetics of Iron Oxide Pellets with H2 and CO Mixtures. *International Journal of Minerals, Metallurgy, and Materials* 22, 7 (July 2015), 688–696. https://doi.org/10.1007/s12613-015-1123-x